Unsteady Flow Concepts for Dynamic Stall Analysis

L E Ericsson* and J P Reding†
Lockheed Missiles & Space Company, Sunnyvale, California

It is well established that there is a strong coupling between airfoil motion and boundary layer separation with attendant vortex shedding Unsteady flow mechanisms that influence this dynamic stall event have been described previously Until now sufficient information has not been available to determine the relative importance of various unsteady flow effects, such as the time varying inviscid pressure gradient and the unsteady viscous boundary condition at the wall, the moving wall effect Recent experimental results provide the needed information, revealing how the mode of oscillation for the airfoil determines which unsteady flow effect will dominate

Nomenclature

c = chord length
f = frequency
K_a = dynamic overshoot parameter, Eqs. (5 7)
l = section lift, coefficient $c_l = l/(\rho_\infty U_\infty^2/2)c$
M = Mach number
m_p = section pitching moment, coefficient $c_m = m_p/(\rho_\infty U_\infty^2/2)c^2$
q = pitch rate
Re = Reynolds number based on chord length, $= U_\infty c/\nu_\infty$
r_N = nose radius
t = time
U = axial velocity
u = local velocity
x = chordwise distance from the leading edge
z = translatory coordinate, positive downward
α = angle of attack
$\tilde{\alpha}$ = equivalent angular amplitude, Eq (1)
α_0 = mean (trim) angle of attack
Δ = increment or amplitude
θ = perturbation in pitch
ν = kinematic viscosity
ξ = dimensionless x coordinate, $= x/c$
ρ = air density
ρ_N = dimensionless nose radius, $= r_N/c$
τ = dimensionless time, $= Ut/c$
$\Delta\phi$ = phase lag, $= \omega\Delta t = \tilde{\omega}\Delta\tau$
ω = angular frequency, $= 2\pi f$
$\tilde{\omega}$ = reduced frequency, $= \omega c/U_\infty$

Subscripts

c.g = center of gravity or rotation axis
le = leading edge
max = maximum
min = minimum
N = nose
s = separation
sp = separation point
v = vortex
vg = vortex growth
W = wall
w = wake
$1\ 2$ = numbering subscript
∞ = freestream conditions

Superscript

$\bar{(\ )}$ = time average value, e g , $\bar{c}_l(t)$

Derivative Symbols

$c_{l\alpha} = \partial c_l/\partial\alpha$
$\dot{\alpha} = \partial\alpha/\partial t$

Introduction

SINCE the last check of our unsteady flow concepts for dynamic stall analysis against experimental and numerical results[1] a great number of experimental investigations have been performed with steadily increasing degrees of sophistication According to McCroskey's reviews[2-5] the more and more extensive experiments have served to illustrate the great complexity of the dynamic stall phenomena but have not led to the understanding needed for the development of a satisfactory prediction method. In the present paper the authors examine the available experimental data base and come to a different conclusion The new results[6 10] provide support for critical elements of concepts previously developed for the unsteady flow mechanisms dominating the dynamic stall process [1 11 13] The purpose of this paper is to delineate the important dynamic stall mechanisms and bring them to the attention of theoreticians. Because of the existing simulation problems in dynamic tests, [14 15] further theoretical work is needed At present, prediction of full scale dynamic stall characteristics, in general, can be obtained only through "analytic extrapolation" from subscale dynamic test results using experimental static data for the complete Reynolds number range from the subscale test to full scale flight [16]

Discussion

Many of the recent experiments have been devoted to investigating the often assumed equivalence between pitching and plunging motions According to McCroskey's latest review,[5] our method[1] is the only one that distinguishes between the two motions

Following Carta[7] we express the equivalent angle as follows:

$$\alpha = \alpha_0 + \theta^*$$

$$\theta^* = \tilde{\alpha}\sin\omega t$$

$$\tilde{\alpha} = |\theta| \qquad \text{true pitch}$$

$$\tilde{\alpha} = |\dot{z}|/U_\infty \qquad \text{equivalent pitch} \qquad (1)$$

Presented as Paper 82 1324 at the AIAA 9th Atmospheric Flight Mechanics Conference San Diego Calif Aug 9 11 1982; received Aug 10, 1982; revision received Jan 2 1984

*Senior Consulting Engineer Associate Fellow AIAA
†Staff Engineer Fellow AIAA

In attached flow there will be a difference in the force generated by pitching and plunging motions at the same instantaneous equivalent angle of attack α According to Ref 11 the instantaneous lift will lag the instantaneous angle of attack with

$$\Delta\alpha_w = \xi_w c\dot{\alpha}/U_\infty \tag{2}$$

where $\xi_w = 1\ 5$

This is the complete α lag for the plunging airfoil, i e $\Delta\alpha_{\text{plunge}} = 1\ 5c\dot{\alpha}/U_\infty$. For the pitching airfoil there is a pitch rate induced lift increment $\Delta c_l = c_{l\alpha}(1-\xi_{cg})c\dot{\alpha}/U_\infty$, giving an effective α lag of

$$\Delta\alpha_{\text{pitch}} = \Delta\alpha_w - (1-\xi_{cg})\,c\dot{\alpha}/U_\infty \tag{3}$$

For an airfoil pitching around the 25% chord, $\xi_{cg} = 0\ 25$, one obtains

$$\Delta\alpha_{\text{pitch}} = \Delta\alpha_w - 0\ 75\,c\dot{\alpha}/U_\infty = 0\ 75\,c\dot{\alpha}/U_\infty = 0\ 5\Delta\alpha_{\text{plunge}} \tag{4}$$

Thus, at $\alpha = \alpha_0$ the "up and downstroke" portions of the c_l or c_n loops should be twice as far apart for the plunging as for the pitching airfoil (for the same reduced frequency) Carta's test[7] gave this expected data trend (Fig 1)

The difference between the dynamic stall characteristics is a little more complicated We have discussed in detail[1] how the dynamic overshoot of static $c_{l\max}$ is caused by two viscous flow effects at moderate amplitudes and frequencies (There is an additional effect of the "spilled leading edge vortex" at large amplitudes and high frequencies)[13] One is the integrated effect of the time-lagged external pressure gradient on the boundary layer development, giving

$$\begin{aligned}\Delta c_{ls1} &= c_{l\alpha}\ \Delta\alpha_{s1}\\ \Delta\alpha_{s1} &= K_{a1}\ c\dot{\alpha}/U_\infty\end{aligned} \tag{5}$$

The other is the so called "leading-edge jet" effect (Fig 2). As the airfoil leading edge moves upward the boundary layer between stagnation and separation points experiences a moving wall/wall jet effect very similar to that observed on a rotating cylinder,[17] as is sketched in the inset in Fig 2 Thus, the boundary layer has a fuller profile than in the steady case and, therefore, is more difficult to separate On the "downstroke" the effect is the opposite, promoting separation. It is shown in Refs 1 and 11 how this effect is in a first approximation proportional to $\dot{z}_{le}$ That is,

$$\begin{aligned}\Delta c_{ls2} &= c_{l\alpha}\ \Delta\alpha_{s2}\\ \Delta\alpha_{s2} &= K_{a2}\dot{Z}_{le}/U_\infty\end{aligned} \tag{6}$$

For the airfoil pitching around ξ_{cg} one obtains

$$\begin{aligned}\Delta c_{ls} &= c_{l\alpha}\Delta\alpha_s\\ \Delta\alpha_s &= K_a c\alpha/U_\infty\\ K_a &= K_{a1} + K_{a2}\ \xi_{cg}\end{aligned} \tag{7}$$

These two mechanisms, Eqs (5) and (6), which combine to give Eq (7) for the pitching airfoil, are proportional to the dimensionless pitch and plunging rates, with the effects being opposite on the downstroke to what they are on the upstroke. Recent experimental results[8] for pitch oscillations around the static stall angle are in agreement with this "prognostication"[1 11 12] for low to moderate frequencies (Fig 3) Thus, $(c_l)_{\max}$ grows and $(c_l)_{\min}$ decreases almost linearly with $\tilde{\omega}$ at rates of approximately equal magnitude That is, Eq (7) is valid for both the upstroke, $c\dot{\alpha}/U_\infty > 0$, and the downstroke, $c\dot{\alpha}/U_\infty < 0$, of an airfoil describing oscillations through the stall region

Combining Eqs (1) and (5) one finds that the pressure gradient-lag effect is the same for pitching and plunging airfoils. However, the "leading edge jet" effects are of opposite kind, delaying separation for the pitching airfoil and promoting it for the plunging airfoil

A vivid demonstration of the opposite leading edge jet effects in pitching and plunging motions is provided by the experimental moment characteristics[10 18] in Fig 4 which show how the favorable effects for the pitching airfoil[18] delay stall almost to the end of the cycle, while the plunging airfoil[10] stalls much earlier because of the adverse leading edge jet effects For the plunging airfoil, the leading edge jet effect is zero at the midportion, $\alpha = \alpha_0 = 15$ deg, and reaches peak magnitude at the end point, $\alpha = 15$ deg $\pm$ 10 deg The effect is adverse at high angles of attack, 15 deg $< \alpha < 25$ deg, and favorable at low angles, 5 deg $< \alpha < 15$ deg In contrast, the pitching airfoil experiences the peak leading-edge jet effect at midpoint, favorable on the upstroke and adverse on the downstroke, with the effect becoming zero at the end points This explains the difference between the two loops in Fig 4 Similar results have been obtained by Carta [7]

At stall a vortex is shed from the leading edge and travels downstream over the chord For high-frequency oscillations this "spilled vortex" remains over the airfoil a significant portion of the cycle If the oscillation amplitude is large so that $\dot{\alpha}c/U_\infty$ becomes of significant magnitude, the lift induced by the vortex can be large It is larger the larger the angle of attack is at the time of vortex shedding [13] Thus, the different stall angles for pitching and plunging airfoils result in vortex induced lift of widely differing magnitudes This is well illustrated by the results obtained by Maresca et al ,[10] who designed plunging tests in accordance with Eq (1) to provide the "equivalent pitch" results to be compared with the true pitch data obtained by Carr et al [18] (Fig 5) The original results have been zero-shifted to agree in the early attached flow portion of the upstroke One expects this agreement since there are no significant viscous flow effects and the pitch rate induced effects discussed earlier are zero at the end of the cycle

From Fig 4 one obtains the values of 17 and 24 deg for the vortex shedding on the plunging and pitching airfoils, respectively According to Ref 13, the vortex induced lift is proportional to $\sin^2$ of these angles That is, it would be twice

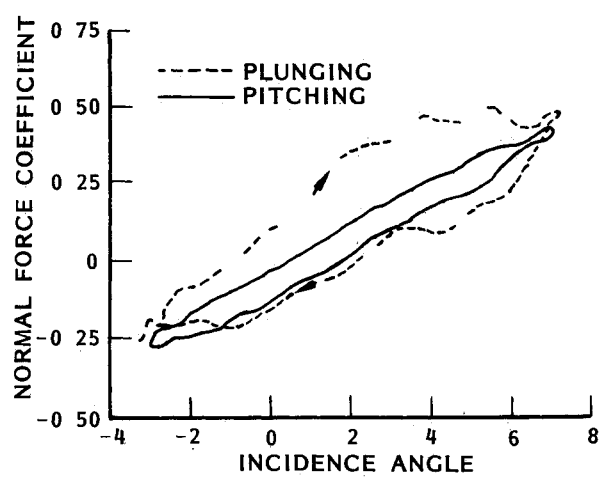

Fig 1 Normal force loops for $\alpha_0 = 2$ deg, $\tilde{\alpha} = 5$ deg and $\tilde{\omega} = 0\ 5$ (Ref 7)

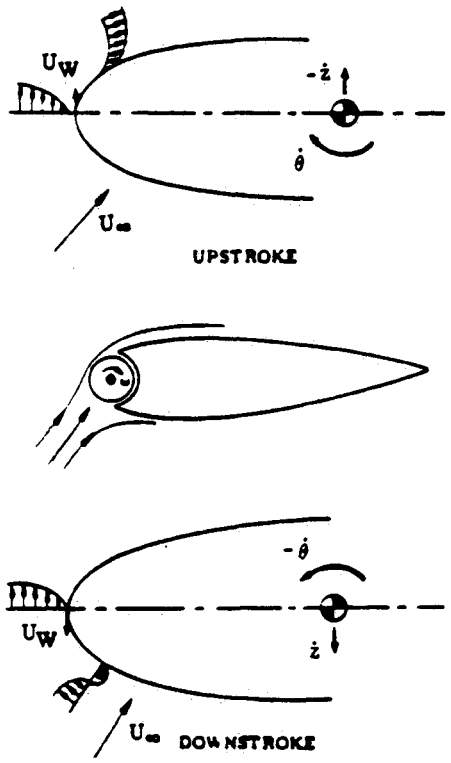

Fig 2 Leading edge jet effect

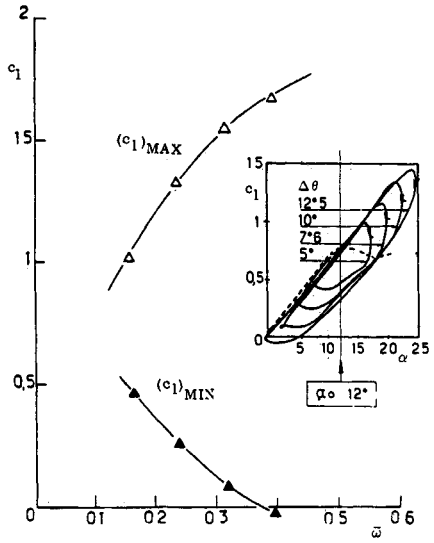

Fig 3 Effect of reduced frequency on maximum and minimum lift [8]

as large for the pitching as for the plunging airfoil, which is in good agreement with the experimental data trend in Fig 5

Accelerated Flow Effects

In Fig 6 the time-average lift measured by Maresca et al [9] on an NACA 0012 airfoil, describing streamwise oscillations of amplitude $\Delta x/c=0.565$, is shown as a function of (trim) angle of attack for different reduced frequencies It can be seen that for $\bar{\omega}>0\,656$ the stall induced lift loss is not realized It is described in Ref 13 how this is the result of viscous time lag effects which allow the flow to reattach in the nose region, where the main lift generation occurs, before the "spilled leading-edge vortex" has passed downstream of the trailing edge of the airfoil In dimensionless form the viscous time lag $\Delta\tau=\Delta t/(c/U_\infty)$ is as follows:

$$\Delta\tau=\xi_s+\xi_{sp}+\xi_{vg}+\xi_v \qquad (8)$$

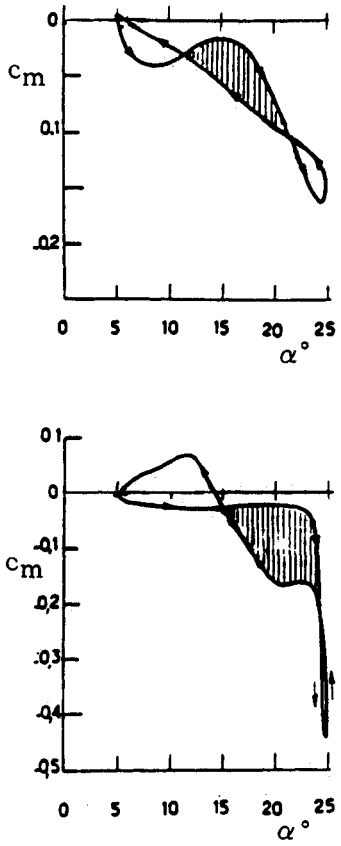

Fig 4 Moment loops for plunging and pitching oscillations

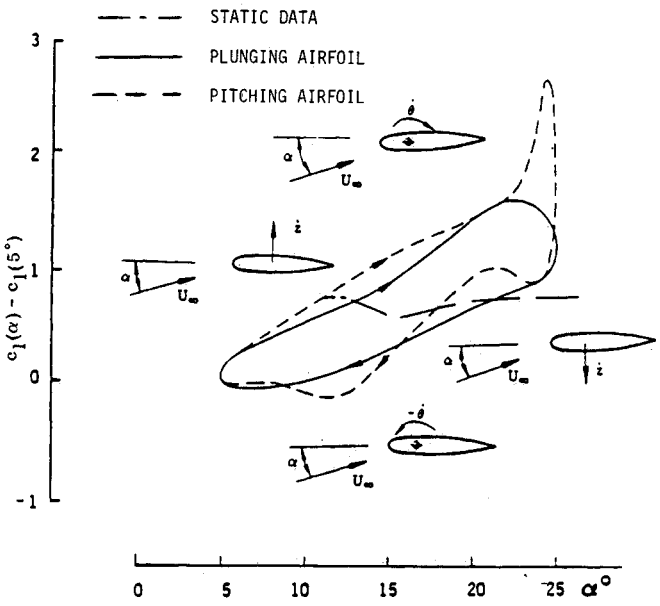

Fig 5 Comparison of lift loops for plunging and pitching airfoils

where $\xi_s=K_{al}$ of Eq (5), with $K_{al}\approx 2$ for the NACA 0012 airfoil ξ_{sp} is the effect of the moving separation point where, according to the results of McCroskey et al ,[19] only the turbulent value $\xi_{sp}=0\,75$ is of practical interest ξ_{vg} is the vortex growth phase of the spilled vortex, as described in Ref 13 using Carta's detailed measurements,[20] with $\xi_{vg}\approx 0\,9$ for the NACA 0012 airfoil $\xi\approx 1\,8$ is the (dimensionless) time required for the vortex to travel to the trailing edge [13]

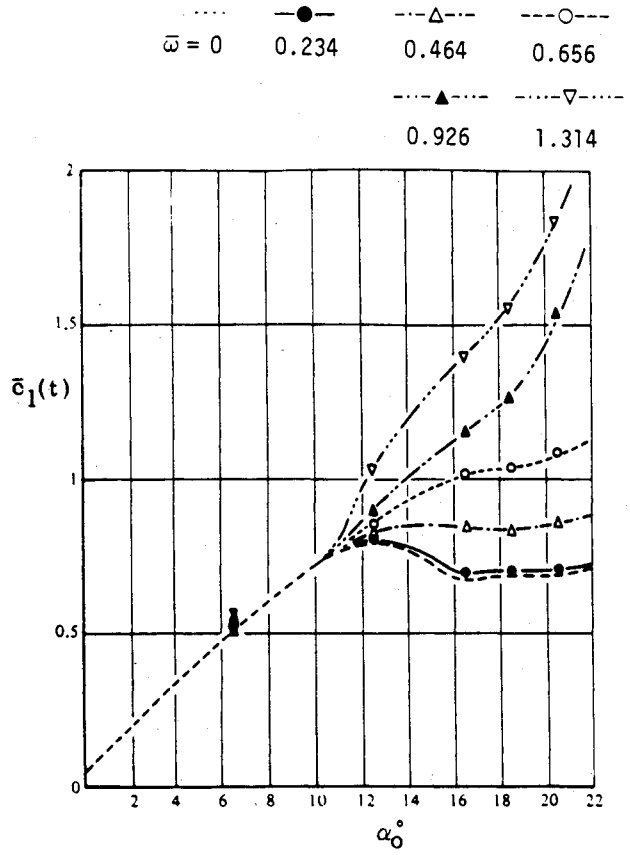

Fig. 6 Time-average lift for streamwise airfoil oscillation of amplitude $\Delta x/c = 0.565$ (Ref. 9).

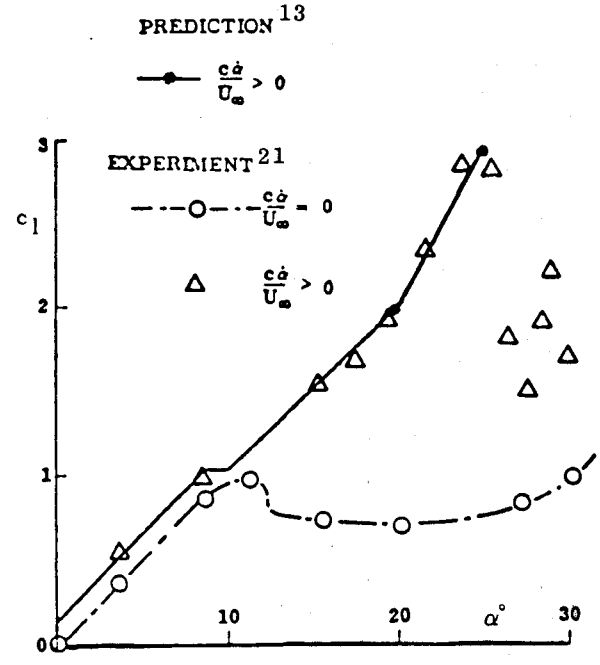

Fig. 7 Effect on lift of rampwise α change.

Thus, the phase lag corresponding to the time lag $\Delta\tau$ is

$$\Delta\phi = \bar{\omega}\Delta\tau = 5.45\bar{\omega} \tag{9}$$

When $\Delta\phi > \pi$, flow reattachment will occur at the bottom of the cycle before the spilled leading-edge vortex has left the airfoil, i.e., for $\bar{\omega} > 0.58$, according to Eq. (9). This is in good agreement with the experimental results[9] in Fig. 6. When $\bar{\omega}$ is increased further the lift from the spilled leading-edge vortex

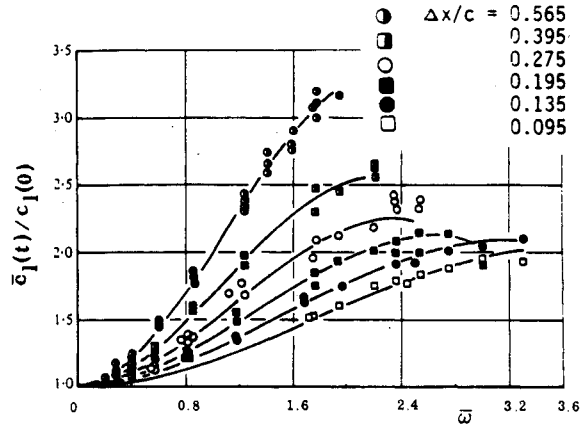

Fig. 8 Effect on time-average lift of the amplitude and frequency of streamwise airfoil oscillations at $\alpha_0 = 20$ deg.[9]

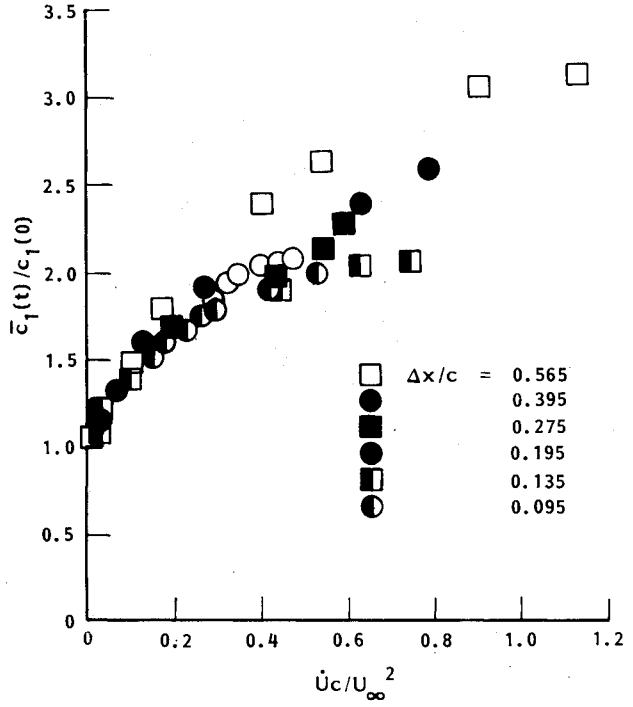

Fig. 9 Effect of normalized acceleration parameter on time average lift.

is added to a more and more fully developed attached flow lift on the airfoil leading-edge, resulting in an increased time-average lift as is shown in Fig. 6. Figure 7 shows this spilled vortex effect on the instantaneous lift, measured[21] and computed[13] for an NACA-0012 airfoil describing a rampwise increase of the angle of attack. Figure 8 summarizes the effect of amplitude and frequency of the streamwise oscillation on the overshoot of the time-average lift above the static value.[9] The effects of amplitude and frequency can be combined to form the dimensionless acceleration parameter $\dot{U}c/U_\infty^2$, used by Minkkinen et al.[22] In the present case one obtains

$$|\dot{U}c/U_\infty^2| = \bar{\omega}^2 \Delta x/c \tag{10}$$

This permits the experimental results[9] in Fig. 8 to be represented as shown in Fig. 9. That is, the data collapse to an initial linear growth of

$$\bar{c}_l(t)/c_l(0) \approx 1.0 + 4|\dot{U}c/U_\infty^2| \tag{11}$$

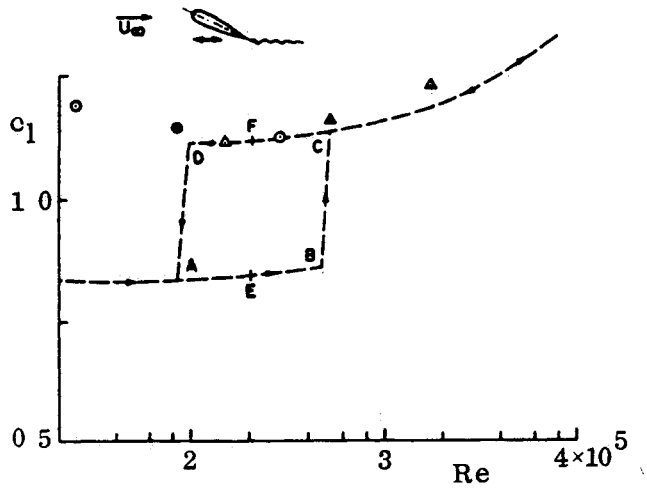

Fig 10 Hysteresis effects for an airfoil oscillating with a streamwise amplitude $\Delta x/c = 0\ 565$ (Ref. 23)

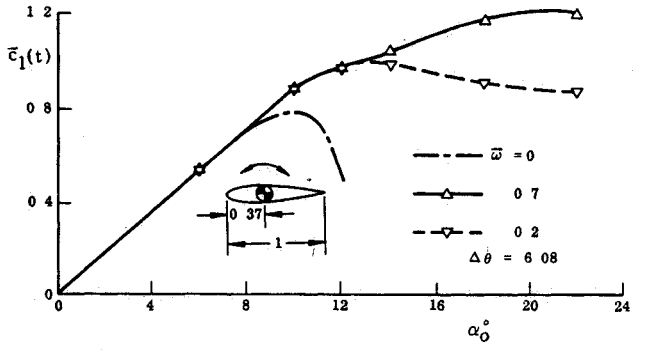

Fig 11 Time-average lift for a thin airfoil describing pitch oscillations at $Re = 10^6$ (Ref. 24)

approaching asymptotic limits for high frequency which increase with increasing amplitude, $\Delta x/c$ The asymptotic results are in good qualitative agreement with the peak lift measured on an NACA 0012 airfoil describing a rampwise change of angle of attack[21] (Fig 7)

After the above discussion of accelerated flow effects the experimental results by Maresca et al ,[23] shown in Fig 10, no longer appear so remarkable After starting the oscillations at the stalled condition, E in Fig 10, Maresca et al.[23] found that when stopping the oscillations the lift remained at the at tached flow level, F in Fig 10 This is the obvious con sequence of the accelerated flow effects just discussed The old results by Halfman et al [24] were really more perplexing, showing that attached flow could be established for pitching oscillations in the deep stall region even when the oscillation never "reached down" to the static stall angle (Fig 11) For example, at $\alpha_0 = 22$ deg the minimum instantaneous angle of attack is $\alpha_0 - \Delta\theta = 15\ 92$ deg, well above the static stall angle, $\alpha_s < 12$ deg The similarity in trends are evident in comparing Figs 9 and 11 The results in Fig 11 prompted our discovery of the leading-edge jet effect [1]

Recent experiments[25,26] have provided the instructive results shown in Fig 12 In Fig 12a the α time history for stall penetration is closely simulated for two oscillations with different trim angle α_0, amplitude $\Delta\theta$, and reduced frequency $\bar{\omega}$ That the lift stall characteristics are almost identical, as are also the moment characteristics,[25,26] is hardly surprising Somewhat more interesting is the comparison in Fig. 12b between the results for two oscillations around the same α_0 with different amplitude $\Delta\theta$ and frequency $\bar{\omega}$ but with the same product $\Delta\theta\bar{\omega}$ As long as the dynamic stall occurs well before the end of the upstroke, the α time history at stall will be the same for the two oscillation cases and the dynamic $c_{l\max}$ will be the same, as is illustrated by the results in Fig 12b $c_{l\text{peak}}$ is not reached until the dimensionless time increment $\Delta\tau = \xi_{sp} + \xi_{vg} + 0\ 7\xi_v = 2.91$ after that dynamic stall has occurred Applying the prediction method of Ref 13 one obtains $c_{l\text{peak}} = 2\ 17$ and $2\ 13$ for the low and high-frequency oscillations, respectively This is in satisfactory agreement

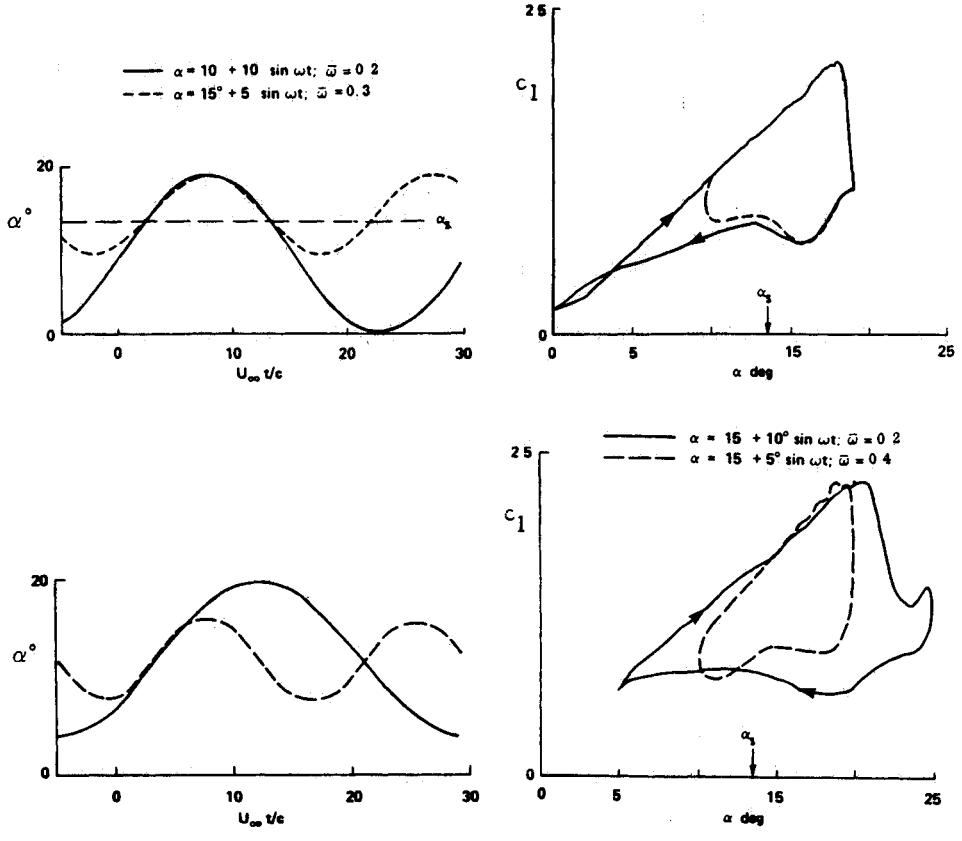

Fig 12 Dynamic lift on the SC 1095 airfoil [25]

with the experiments considering the data accuracy indicated in Ref 22

It should be emphasized that the results in Fig 12 are obtained only for large amplitude/low frequency oscillations where the behavior at stall is almost the same as for a ramp wise α change At higher frequencies the phase lag characteristics become important For example, for $\bar{\omega}=0\ 68$ and $\Delta\theta=6$ deg in Ref 27, which gives $\Delta\theta\bar{\omega}=0\ 071$, the phase angle $\bar{\omega}\Delta\tau$ became so large that flow reattachment occurred at the leading edge before the spilled vortex passed downstream of the trailing edge [13] The same value $\Delta\theta\bar{\omega}=0\ 071$ can be obtained with $\bar{\omega}=0\ 30$ and $\Delta\theta=13\ 6$ deg, for which the lift stall loop would be very similar to those in Fig 12, which do show full dynamic stall effects

Utilization of Subscale Test Data

For the foreseeable future the prediction of dynamic stall characteristics will depend heavily upon the use of experimental results, usually obtained on subscale models. Great care has to be exercized when using the data for prediction of full scale dynamic characteristics They can be used most effectively by applying the analytic extrapolation method described in Ref 16 Detailed experimental investigations, such as those performed by Maresca et al.,[8 10 23] Carta,[7 20] and McCroskey et al ,[6 18 28] provide the detailed description of the unsteady flow needed to guide theoretical research

Conclusions

Examining previously developed unsteady flow concepts for dynamic stall analysis in light of recent experimental results reveals the following

1) The new experimental results prove conclusively the existence of the so called "leading-edge jet" effect, which can explain the observed differences between plunging and pitching airfoil characteristics.

2) Experimental results for inclined airfoils describing streamwise oscillations in steady flow, or subjected to an accelerating mean flow, support the earlier postulated linear dependence of dynamic stall overshoot on the dimensionless time rate of change of the angle of attack, $c\dot{\alpha}/U_\infty$

3) The assumed algebraic dependence of the above two effects on $c\dot{\alpha}/U_\infty$, including the reversal of the effects when $\dot{\alpha}$ changes sign, is verified by recent experimental results

The main conclusion to be drawn from this study is that, thanks to recent experimental results, the unsteady flow mechanisms that have decisive influence on dynamic stall characteristics can be described with the detail needed to help focus future research on the vital flow phenomena

References

[1] Ericsson L E and Reding, J P Dynamic Stall Analysis in Light of Recent Numerical and Experimental Results *Journal of Aircraft*, Vol 13, April 1976 pp 248 255

[2] McCroskey, W J 'Recent Developments in Dynamic Stall *Proceedings of the University of Arizona/USAF OSR Symposium on Unsteady Aerodynamics* Tuscon Ariz edited by R B Kinney March 1975, pp 1 33

[3] McCroskey, W J Some Current Research in Unsteady Aerodynamics—A Report from the Fluid Dynamics Panel ' Paper 24 46th Meeting of AGARD Propulsion and Energetics Panel Monterey Calif , Sept 1975

[4] McCroskey, W J Prediction of Unsteady Separation Flows on Oscillating Airfoils AGARD LS 94 Feb 1978

[5] McCroskey, W. J The Phenomenon of Dynamic Stall, NASA TM 81264 and Paper 2 VKI Lecture Series 1981 4, March 1981

[6] McAlister K W Carr L W and McCroskey W. J , Dynamic Stall Experiments on the NACA 0012 Airfoil NASA TP 1100, Jan 1978

[7] Carta F O A Comparison of the Pitching and Plunging Response of an Oscillating Airfoil,' NASA CR 3172, Oct 1979.

[8] Favier D Rebont, J and Maresca, C Profil d Aile a Grande Incidence Animé d un Mouvement de Pilonnement *16eme Colloque d'Aerodynamique Appliquee* Lille Nov 1979

[9] Maresca, C Favier D and Rebont J , 'Experiments on an Airfoil at High Angle of Incidence in Longitudinal Oscillations ' *Journal of Fluid Mechanics* Vol 92 1979 Pt 4 pp 671 690

[10] Maresca C A , Favier D J , and Rebont J M Unsteady Aerodynamics of an Airfoil at High Angle of Incidence Performing Various Linear Oscillations in a Uniform Stream ' *Journal of the American Helicopter Society* Vol 13 April 1981 pp 40 45

[11] Ericsson, L E and Reding J P Unsteady Airfoil Stall Review and Extension *Journal of Aircraft* Vol 8 Aug 1971 pp 609 616

[12] Ericsson L E and Reding, J P 'Quasi Steady and Transient Dynamic Stall Characteristics '' Paper 24 AGARD CP 204 Sept 1976

[13] Ericsson L E and Reding J. P., Dynamic Stall at High Frequency and Large Amplitude' *Journal of Aircraft* Vol 17 March 1980 pp 136 142

[14] Ericsson, L E. and Reding, J. P 'Dynamic Stall Simulation Problems ' *Journal of Aircraft* Vol 8 July 1971 pp 579 583

[15] Ericsson L E and Reding J P 'Scaling Problems in Dynamic Tests of Aircraft Like Configurations ' Paper 25 AGARD CP 227 Sept 1977

[16] Ericsson L. E and Reding, J P , Analytic Extrapolation to Full Scale Aircraft Dynamics ' Journal of Aircraft Vol 21 March 1984, pp 222 224.

[17] Ericsson, L E ' Karman Vortex Shedding and the Effect of Body Motion, *AIAA Journal*, Vol 18, Aug. 1980 pp 935 944

[18] Carr L W , McAlister, K W and McCroskey, W J Analysis of Development of Dynamic Stall Based on Oscillating Airfoil Experiments, ' NASA TN D8382, 1977

[19] McCroskey, W J Carr L W and McAlister K W Dynamic Stall Experiments on Oscillating Airfoils *AIAA Journal* Vol. 14 Jan 1976 pp 57 63.

[20] Carta, F. O., ' Analysis of Oscillatory Pressure Data Including Dynamic Stall Effects ' NASA CR 2394, May 1974

[21] Ham N. D and Garelick M S., 'Dynamic Stall Considerations in Helicopter Rotors *Journal of the American Helicopter Society*, Vol. 13 April 1968 pp 44 45

[22] Minkkinen, G T Wilson T A and Beavers, G S , An Experiment on the Lift of an Accelerated Airfoil *AIAA Journal* Vol. 14 May 1976, pp 687 689

[23] Maresca C , Rebont J , and Valensi J , Separation and Reattachment of the Boundary Layer on a Symmetric Airfoil Oscillating at a Fixed Incidence in Steady Flow *Proceedings of the University of Arizona/USAF OSR Symposium on Unsteady Aerodynamics* Tuscon Ariz edited by R B Kinney 1975 pp 35-54

[24] Halfman, R L Johnson H C and Haley S M Evaluation of High Angle of Attack Aerodynamic Derivative Data and Stall Flutter Prediction Techniques ' NACA TN 2533 Nov 1951

[25] McCroskey W J., McAlister K W Carr, L W., Pucci S. L., Lambert O and Indergrand R F Dynamic Stall on Advanced Airfoil Sections *Journal of the American Helicopter Society*, Vol. 13, July 1981 pp 40 50

[26] McCroskey W J and Pucci, S L Viscous Inviscid Interaction on Oscillating Airfoils in Subsonic Flow, *AIAA Journal* Vol 20 Feb 1982 pp 167 174

[27] McCroskey W J and Philippe, J J , Unsteady Viscous Flow on Oscillating Airfoils ' AIAA Paper 74 182 Jan 1974

[28] McCroskey W J McAlister, K W Carr L W and Pucci S L An Experimental Study of Dynamic Stall on Advanced Airfoil Sections: Volume 1, Summary of the Experiment NASA TM 84245, July 1982